International Journal of
Environmental Research and Public Health

MDPI

Article

Chemical Composition, Sources, and Health Risk Assessment of $PM_{2.5}$ and PM_{10} in Urban Sites of Bangkok, Thailand

Mushtaq Ahmad [1,2], Thanaphum Manjantrarat [1], Wachiraya Rattanawongsa [3], Phitchaya Muensri [3], Rattaporn Saenmuangchin [3], Annop Klamchuen [3], Sasitorn Aueviriyavit [3], Kanokwan Sukrak [1], Wiyong Kangwansupamonkon [3,4,*] and Sirima Panyametheekul [1,5,6,*]

1 Department of Environmental Engineering, Faculty of Engineering, Chulalongkorn University, Bangkok 10330, Thailand
2 State Key Joint Laboratory of Environment Simulation and Pollution Control, School of Environment, Beijing Normal University, Beijing 100875, China
3 National Nanotechnology Center (NANOTEC), National Science and Technology Development Agency, Pathum Thani 12120, Thailand
4 AFRS(T) The Royal Society of Thailand, Sanam Sueapa, Dusit, Bangkok 10300, Thailand
5 Thailand Network Center on Air Quality Management: TAQM, Chulalongkorn University, Bangkok 10330, Thailand
6 Research Unit: HAUS IAQ, Chulalongkorn University, Bangkok 10330, Thailand
* Correspondence: wiyong@nanotec.or.th (W.K.); sirima.p@chula.ac.th (S.P.); Tel.: +66-2-5647100 (ext. 6550) (W.K.); +66-2218-6667 (S.P.)

Citation: Ahmad, M.; Manjantrarat, T.; Rattanawongsa, W.; Muensri, P.; Saenmuangchin, R.; Klamchuen, A.; Aueviriyavit, S.; Sukrak, K.; Kangwansupamonkon, W.; Panyametheekul, S. Chemical Composition, Sources, and Health Risk Assessment of $PM_{2.5}$ and PM_{10} in Urban Sites of Bangkok, Thailand. *Int. J. Environ. Res. Public Health* **2022**, *19*, 14281. https://doi.org/10.3390/ijerph192114281

Academic Editor: Maria José Rosa

Received: 5 October 2022
Accepted: 27 October 2022
Published: 1 November 2022

Abstract: Of late, air pollution in Asia has increased, particularly in built-up areas due to rapid industrialization and urbanization. The present study sets out to examine the impact that pollution can have on the health of people living in the inner city of Bangkok, Thailand. Consequently, in 2021, fine particulate matter ($PM_{2.5}$) and coarse particulate matter (PM_{10}) chemical composition and sources are evaluated at three locations in Bangkok. To identify the possible sources of such particulates, therefore, the principal component analysis (PCA) technique is duly carried out. As determined via PCA, the major sources of air pollution in Bangkok are local emission sources and sea salt. The most significant local sources of $PM_{2.5}$ and PM_{10} in Bangkok include primary combustion, such as vehicle emissions, coal combustion, biomass burning, secondary aerosol formation, industrial emissions, and dust sources. Except for the hazard quotient (HQ) of Ni and Mn of $PM_{2.5}$ for adults, the HQ values of As, Cd, Cr, Mn, and Ni of both $PM_{2.5}$ and PM_{10} were below the safe level (HQ = 1) for adults and children. This indicates that exposure to these metals would have non-carcinogenic health effects. Except for the carcinogenic risk (HI) value of Cr of $PM_{2.5}$ and PM_{10}, which can cause cancer in adults, at Bangna and Din Daeng, the HI values of Cd, Ni, As, and Pb of $PM_{2.5}$ and PM_{10} are below the limit set by the U.S. Environmental Protection Agency (U.S. EPA). Ni and Mn pose non-carcinogenic risks, whereas Cr poses carcinogenic risks to adults via inhalation, a serious threat to the residents of Bangkok.

Keywords: air pollution; fine and coarse particles; risk assessment; source apportionment; principal component analysis

1. Introduction

Globally, particulate matter (PM) levels are increasing rapidly, with most cases occurring in the developing world and causing significant health and environmental implications [1]. PM pollution is one of the significant global risks to human health. Current global air quality regulations aim to decrease the concentrations of $PM_{2.5}$ and PM_{10}, as well as the chemical composition associated with adverse health implications [2]. The population in Asia has increased due to rapid industrialization, and, thus, energy consumption has also increased with population expansion. Major air pollutants have been emitted in urban

areas, intensified by climatic and topographical conditions that frequently inhibit the dispersion of pollutants in metropolitan regions [3,4]. Identifying the chemical composition, sources, and toxicity of PM has become essential.

The chemical composition of PM can vary significantly due to the influence of emission sources, weather conditions, and the possibility of dispersion [5,6]. The carbonaceous components of PM primarily consist of elemental carbon (EC) and organic carbon (OC), which account for approximately 10 and 45% of the mass of $PM_{2.5}$ and PM_{10}, respectively [7,8]. One of the common components of atmospheric particles is water-soluble inorganic species (WSIS). Meteorological and geographical conditions, industrial particle emissions, transportation, agricultural practices, and natural sources significantly influenced WSIS [9]. Heavy metals are poorly biodegradable, carcinogenic, and contribute less to the mass of $PM_{2.5}$ and PM_{10}. When humans are exposed to high doses of heavy metals for a long period, the heavy metals become toxic [10].

Human health and well-being are considered to be dependent on clean air. Air quality standards have been set in many countries to protect the public's health. These standards have become more important to environmental policies and national risk management [11]. Due to the high concentration of atmospheric $PM_{2.5}$ and PM_{10}, epidemiological studies have demonstrated that humans are exposed to a serious risk of respiratory and cardiovascular diseases [12]. Several studies have found strong evidence that exposure to PM has directly caused cardiopulmonary and ischemic heart disease-related mortality [13]. The size and composition of particulate matter determine its toxicity. Researchers have found that particle composition might have a greater impact than particle size in some cases [14,15]. In addition to its adverse impacts on physical health that have been extensively studied, PM pollution also significantly impacts the economy [16,17].

In this paper, the carcinogenic and non-carcinogenic effects of metals and metalloids on adults and children have been estimated using U.S. EPA methodologies. During the wintertime, the high concentration of toxic metals in $PM_{2.5}$ poses serious carcinogenic (HI) and non-carcinogenic (HQ) risks via inhalation exposure to the residents of Lahore and Peshawar [18]. In urban parks in Beijing, the non-carcinogenic (HQ) risk of heavy metals via inhalation exposure was below the safe level (HQ = 1) in road dust; however, the HI values of heavy metals for children were higher than for adults [19]. The study aims to chemically characterize $PM_{2.5}$ and PM_{10} at the urban sites of Bangkok (Ari, Din Daeng, and Bangna) in order to identify possible sources. The principal component analysis (PCA) method has been duly carried out. The carcinogenic and non-carcinogenic risks of heavy metals via inhalation exposure have been evaluated in the study area. Thus, the results of this study will provide health professionals and the general public with a better understanding of air quality, eliciting a sense of awareness about the toxicity of metal-bounded particles and how to control them.

2. Materials and Methods

2.1. Study Area and Sampling

For the monitoring of $PM_{2.5}$ and PM_{10}, three sampling locations in Bangkok were selected: (1) Ari, (2) Din Daeng, and (3) Bangna. In Figure 1, the map of the sampling locations is shown.

2.1.1. Ari (13°46′59.6″ N 100°32′25.8″ E)

This station is in the Pollution Control Department area. The height of air sampling equipment is 5 m above ground level. This area is surrounded by government office buildings, such as the Treasury Department, Ministry of Finance, Revenue Department, Ministry of Natural Resources and Environment, Department of Water Resources, Department of Environmental Quality Promotion, and Institute of Public Relations. In addition, this station is in an area with dormitories and condominiums. Ari was designated as the representative of the residential area in the city.

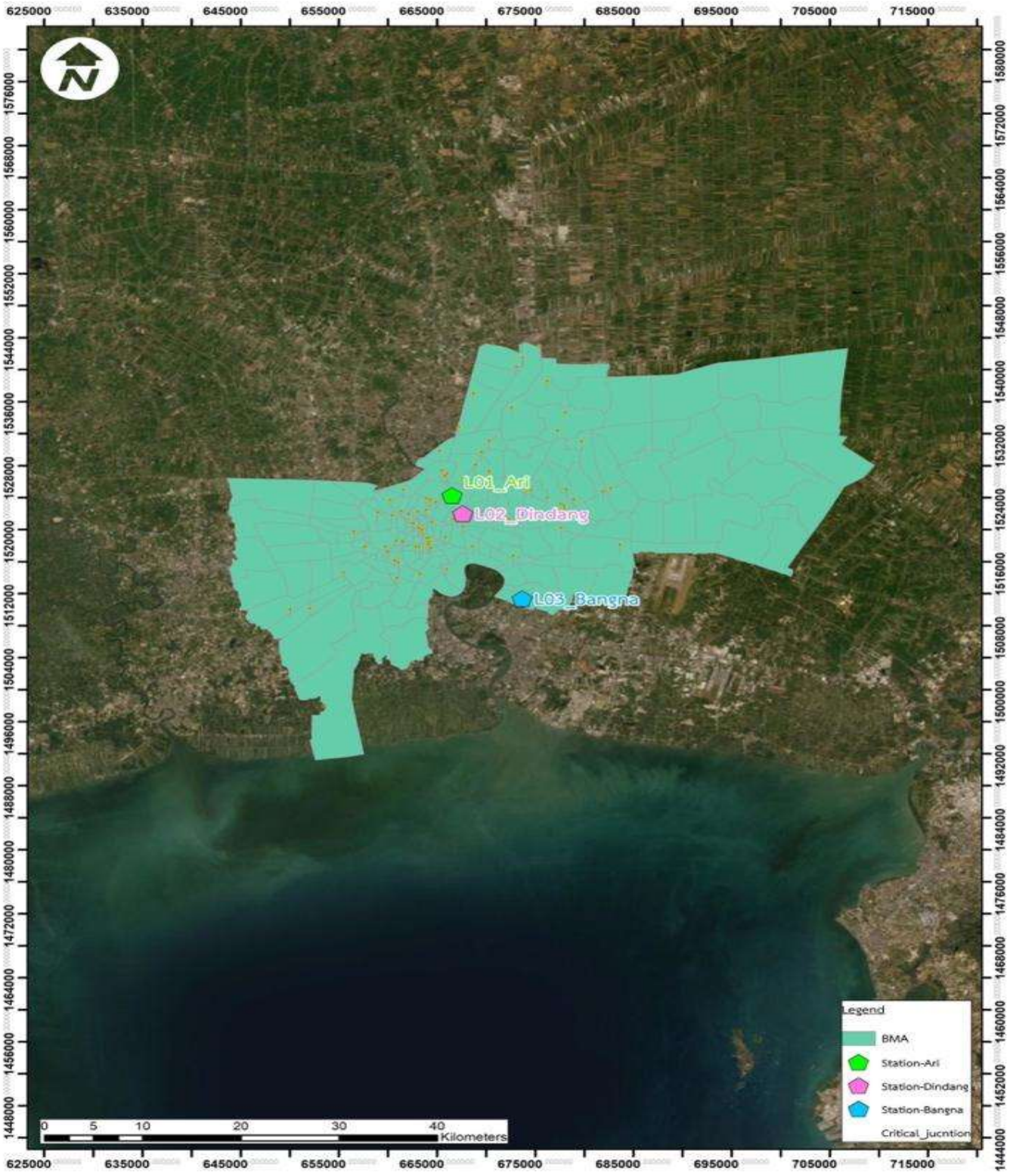

Figure 1. The map of Bangkok metropolitan area, highlighting the sampling locations (Ari, Din Daeng, and Bangna).

2.1.2. Din Daeng (13°45′45.2″ N 100°33′01.1″ E)

The height of air sampling equipment is 5 m above ground level. This station is located next to Din Daeng Road, about 700 m away, opposite the Ministry of Labor. This station represents traffic emissions.

2.1.3. Bangna (13°39′58.8″ N 100°36′20.7″ E)

The height of air sampling equipment is 5 m above ground level. This station is in the Thai Meteorological Department area. According to the Department of Industrial Works website, many factories are located within a 2 km radius, including car paint, metals, plastic packaging production, car repairs, garment factories, wood processing industries, and producing publications.

The samples of $PM_{2.5}$ and PM_{10} were collected every 24 h, at each sampling site, from 8:00 am to 7:00 am (local time) the next day. The samples were collected on quartz fiber filter (PallFlex) by drawing air at a rate of 40 L/min using a Nano-sampler equipped with $PM_{2.5}$ and PM_{10} impactors. At each sampling site, 30 samples of $PM_{2.5}$ and PM_{10} were collected. Before and after sampling, the filters were weighed on an analytical balance and stored for 24 h at a temperature of 25 °C and relative humidity of 50%. The sampled filters were stored in a refrigerator at −40 °C for further analysis.

2.2. Chemical Analysis

The carbonaceous species, water-soluble ions, and metal elements were evaluated in $PM_{2.5}$ and PM_{10} samples. The organic carbon (OC) and elemental carbon (EC) were measured using the thermal/optical reflectance (TOR) method of a DRI THERMAL OPTICAL Carbon Analyzer. To measure OC and EC, the filter punch size of 0.523 cm^2 was heated in a totally oxygen-free helium (He) atmosphere. All OC fractions were released on a filter at four stepwise temperatures of 120 °C (OC1), 250 °C (OC2), 450 °C (OC3), and 550 °C (OC4). EC was measured at 550 °C (EC1), 700 °C (EC2), and 800 °C (EC3), and the pure He was changed to an O_2/He 2% mixture. A laser-monitored optical pyrolyzed carbon (OP). OC was obtained by OC1 + OC2 + OC3 + OC4 + OP, whereas EC was formed by EC1 + EC2 + EC3 − OP.

The water-soluble ions were measured by ultrasonically extracting one quarter of the filter with 10 mL of ultrapure water for 60 min. A Teflon filter (PTFE) with a pore size of 0.45 μm was used to remove the insoluble species of the extract. Next, an electrical conductivity detector examined the water-soluble ions using ion chromatography (ICS–1100). An Ion Pac AS11 connected to an Ion Pac AG23 pre-column was used to separate the anions, Cl^-, $NO_3{}^-$, and $SO_4{}^{2-}$. The cations, $NH_4{}^+$, Na^+, K^+, Mg^{2+}, and Ca^{2+}, were separated with an Ion Pac CS12A analytical column connected to an Ion Pac CG12A pre-column.

Among the metals investigated are Na, Mg, Al, K, Ca, Sc, Ti, V, Cr, Mn, Fe, Co, Ni, Cu, Zn, As, Se, Cd, Ba, Ce, Pt, and Pb. An acid solution of 1.5 mL of HCl, 1.0 mL of HNO_3, and 1.0 mL of HBF_4, diluted with 10 mL of ultrapure water, was prepared. A 10 mL acid solution was used to digest one quarter of each filter. Using a microwave digestion unit, the temperature of the digestion solution was maintained at 170 °C for 10 min (ramping time, 15 min) and then increased to 180 °C for 15 min (ramping time, 20 min). After cooling, the extracted samples were filtered through a cellulose filter with a pore size of 6 μm and diluted with 10 mL of ultrapure water. Inductively coupled plasma-mass spectrometry (Agilent Technologies 7900 ICP-MS, Santa Clara, CA, USA) was used to measure the metals in the solution. To correct the background concentrations of carbonaceous species, ions, and metals, blank filters were measured using the same method as sample filters. The standard chemicals were applied to check the performance of three chemical analysis methods. Glucose standard was used for calibrating the carbon analysis technique and calibration curves of ion, and metal standards were also used for ion and elemental analysis, respectively.

2.3. Estimation of Primary Organic Carbon and Secondary Organic Carbon

The concentration of primary organic carbon (POC) and secondary organic carbon (SOC) was estimated following the EC-tracer method. The minimum OC/EC ratio was

used to estimate POC and SOC in aerosol [20]. The following equations were used to estimate POC and SOC:

$$POC = EC \times \left(\frac{OC}{EC}\right)_{min} \quad (1)$$

$$SOC = OC - POC \quad (2)$$

where OC represents the measured OC concentration; $\left(\frac{OC}{EC}\right)_{min}$ represents the estimated minimum OC/EC ratio.

2.4. Principal Component Analysis (PCA)

Principal component analysis (PCA), one of the receptor models, was used to identify the potential sources of $PM_{2.5}$ and PM_{10} [21]. PCA considers the concentration of a species at a receptor site to represent the sum of the contributions from several sources/factors, as shown as follows:

$$X_{ij} = \sum_{k=1}^{P} g_{ik} f_{kj} + e_{ij} \quad (3)$$

where x_{ij} represented the concentration of jth species in the ith sample, g_{ik} is contribution of the kth factor/source to the ith sample, and f_{kj} represented the relative quantity of the jth species in the kth source. In an ideal situation, e_{ij} should only contain an experimental error. However, in practice, some unexplained and unknown errors may be included. PCA was performed using a statistical package for the social sciences (SPSS). The PCA analysis used the concentrations of the carbonaceous species, ions, and metals as variables.

2.5. Health Risk Assessment of Heavy Metals

The U.S. EPA health risk assessment models were used to estimate heavy metal carcinogenic and non-carcinogenic health risk assessments [22]. The following subsections are the three steps in the process of evaluating health risk.

2.5.1. Estimating Exposure Concentrations

The following equation was used to determine the exposure concentration (ExC) via inhalation [22]:

$$ExC = CA \times ET \times EF \times ED/AT \quad (4)$$

where ExC represents the exposure concentration ($\mu g/m^3$); CA is the concentration of studied heavy metals ($\mu g/m^3$) [23]; ET represents exposure time, which is considered to be 24 h/day; EF represents exposure frequency, and is supposed to be 350 days/year; and ED is exposure duration, and it is assumed to be 24 years for adults and 6 years for children. AT represents the average time, which is ED × 365 days/year × 24 h/day for non-carcinogens, whereas for carcinogens, it is 70 years × 365 days/year × 24 h/day.

2.5.2. Non-Carcinogenic Risk Assessment

After calculating the ExC values, each metal's hazard quotient (HQ) was determined to assess its non-carcinogenic risk:

$$HQ = ExC/(RC \times 1000 \frac{\mu g}{mg}) \quad (5)$$

where the hazard quotient is HQ, the exposure concentration is ExC ($\mu g/m^3$), and the inhalation reference concentration is R*f*C (mg/m^3). An HQ value < 1 indicates that there are no non-carcinogenic effects. Conversely, there is a high chance of non-carcinogenic effects when the HQ values > 1 [22,24].

2.5.3. Carcinogenic Risk Assessment

The following equation can be used to calculate the carcinogenic risk (CR) via inhalation exposure [22]:

$$CR = IUR \times ExC \quad (6)$$

where IUR represents the inhalation unit risk $(\mu g/m^3)^{-1}$. For regulatory purposes, the range of permissible risk is from 10^{-6} (1 in 1,000,000) to 10^{-4} (1 in 100,000) [25]. Cd, As, Cr, and Ni are identified as human carcinogens via inhalation, as reported by the International Agency for Research on Cancer (IARC) [26]. Lead (Pb) is also a toxic metal that increases cancer risk. The R*f*C, IUR, and exposure variables for these models were acquired from the Integrated Risk Information System (IRIS) and the U.S. EPA Regional Screening Levels (RSL).

2.6. Meteorological Parameters

The average data of meteorological parameters such as temperature, wind speed, relative humidity, wind direction, and rainfall were obtained from http://www.wunderground.com (accessed on 21 May 2022). During sampling periods, no rainfall event occurred; thus, the rainfall data were not included. In Figure 2, the weather conditions are depicted. During the sampling period, the temperature ranged from 19.0 to 29.0 °C, with an average value of 25.0 ± 2.2 °C. The relative humidity ranged from 50.6 to 92.0%, with an average value of 69.6 ± 12.9%. Similarly, the windspeed data were in the range of 0.1 to 0.6 m/s, with average value of 0.2 ± 0.1 m/s. The wind directions during the sampling time were north and north-eastern.

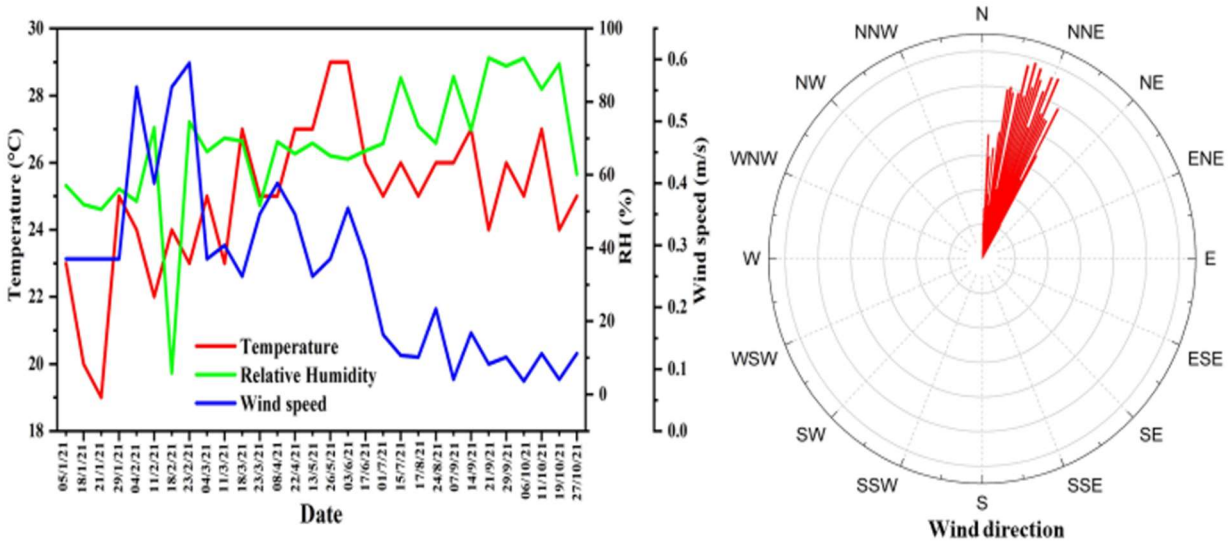

Figure 2. Meteorological parameters, such as temperature, wind speed, relative humidity, and wind direction, during the sampling period in Bangkok metropolitan area, Thailand.

3. Results and Discussion

3.1. Mass Concentration and Composition of $PM_{2.5}$ and PM_{10}

3.1.1. $PM_{2.5}$ and PM_{10} Concentration

Table 1a,b summarizes the mean and range of the mass concentrations of $PM_{2.5}$ and PM_{10} and their carbonaceous, ionic, and metallic/elemental species for sampling sites: Ari, Din Daeng, and Bangna, Bangkok, Thailand. Figure 3 depicts the temporal variation of $PM_{2.5}$ and PM_{10} and their carbonaceous species in sampling sites. The average concentration of $PM_{2.5}$ in Ari was (27.8 ± 16.1) $\mu g/m^3$, Din Daeng (31.3 ± 18.9) $\mu g/m^3$ and Bangna (26.8 ± 14.7) $\mu g/m^3$, whereas PM_{10} was 24.0 ± 8.9 $\mu g/m^3$ (Ari), 30.1 ± 9.9 $\mu g/m^3$ (Din Daeng) and 23.3 ± 7.8 $\mu g/m^3$ (Bangna). The daily concentration of $PM_{2.5}$ exceeded the permissible limit of the WHO guideline (15 $\mu g/m^3$) for almost 90% of the sampling days. In contrast, the concentration of PM_{10} was within the permissible limits. From November 2008 to May 2009, the average concentration of $PM_{2.5}$ in Bangkok at Din Daeng, Bamsomdet, and Chulalongkorn University was 54.9 $\mu g/m^3$, 45.7 $\mu g/m^3$, and 20.3 $\mu g/m^3$. The PM_{10} concentration was 81.5 $\mu g/m^3$, 71.3 $\mu g/m^3$, and 29.7 $\mu g/m^3$; such results are

found to be higher than the current study [27]. Another study carried out in Bangkok from 2003 to 2007 also found that the annual concentration of PM_{10} was higher than in the current study [28]. The average concentration of $PM_{2.5}$ was reported in the residential area (50.3 $\mu g/m^3$), university area (32.8 $\mu g/m^3$), industrial zone (44.5 $\mu g/m^3$), and agricultural zone (29.5 $\mu g/m^3$) of Khon Kaen province in Thailand. These results are slightly higher than in the current study [29].

Table 1. (**a**) Mean and range with standard deviations of the chemical species: $PM_{2.5}$ at Ari, Din Daeng, and Bangna, Bangkok, Thailand (**b**) Mean and range with standard deviations of the chemical species: PM_{10} at Ari, Din Daeng, and Bangna, Bangkok, Thailand.

(**a**)						
	Ari	**Din Daeng**	**Bangna**		**Ari**	**Din Daeng**
	Mean ± Stdv	**Range**	**Mean ± Stdv**		**Mean ± Stdv**	**Range**
	$PM_{2.5}$, Carbonaceous Species, and Ions ($\mu g/m^3$)					
PM	27.8 ± 16.1	7.4–63.0	31.3 ± 18.9	9.1–69.1	26.8 ± 14.7	8.1–55.8
OC	8.4 ± 7.0	1.8–28.2	14.5 ± 7.4	4.2–38.0	8.3 ± 6.7	1.4–24.8
EC	0.7 ± 0.6	0.0–1.9	1.5 ± 1.3	0.1–5.0	0.8 ± 0.7	0.1–3.1
POC	2.6 ± 2.2	0.0–6.9	3.2 ± 2.6	0.2–10.6	2.0 ± 1.7	0.3–7.9
SOC	5.9 ± 5.5	0.0–23.7	11.3 ± 7.1	0.0–33.0	6.3 ± 5.7	0.0–21.1
Na^+	0.4 ± 0.3	0.0–1.1	0.5 ± 0.4	0.0–1.7	0.4 ± 0.4	0.0–1.6
NH_4^+	0.5 ± 0.5	0.0–2.0	0.5 ± 0.5	0.0–1.8	0.4 ± 0.5	0.0–2.0
K^+	0.3 ± 0.3	0.0–1.3	0.3 ± 0.4	0.0–1.7	0.3 ± 0.3	0.0–1.7
Mg^{2+}	0.1 ± 0.1	0.0–0.2	BDL	BDL	0.1 ± 0.1	0.0–0.2
Ca^{2+}	0.2 ± 0.2	0.0–0.8	0.2 ± 0.3	0.0–1.1	0.2 ± 0.2	0.0–0.8
NO_3^-	0.1 ± 0.1	0.0–0.2	0.1 ± 0.1	0.0–0.3	0.1 ± 0.1	0.0–0.3
SO_4^{2-}	0.1 ± 0.1	0.0–0.3	0.2 ± 0.2	0.0–0.6	0.1 ± 0.1	0.0–0.4
Cl^-	0.6 ± 1.1	0.0–5.2	0.6 ± 1.0	0.0–4.7	0.6 ± 1.1	0.0–2.3
	Metals (ng/m^3)					
Na	585.6 ± 855.9	0.0–2446.0	1036.3 ± 1374.4	0.0–5970.3	1255.6 ± 2310.3	0.0–11329.3
Mg	679.8 ± 833.5	0.0–2685.6	704.9 ± 770.5	7.9–3054.2	716.5 ± 785.6	0.0–2542.0
Al	489.9 ± 695.2	0.0–2727.7	853.3 ± 1006.0	0.0–3736.7	988.4 ± 1695.6	0.0–8232.4
K	92.2 ± 198.6	0.0–875.3	201.7 ± 393.2	0.0–1573.6	259.5 ± 539.5	0.0–2563.6
Ca	4586.2 ± 8038.2	0.0–32,000.5	4844.3 ± 8728.0	0.0–35,668.0	4998.1 ± 9410.9	0.0–37,143.8
Sc	42.6 ± 58.0	0.0–191.4	48.4 ± 64.4	0.2–213.5	54.4 ± 69.1	0.2–241.7
Ti	45.4 ± 79.8	0.0–287.2	52.8 ± 75.9	0.6–290.5	54.5 ± 69.5	0.3–244.2
V	0.7 ± 1.3	0.0–4.2	1.2 ± 1.7	0.0–5.5	0.9 ± 1.3	0.0–5.1
Cr	2.6 ± 7.7	0.0–41.9	1.9 ± 3.2	0.0–15.5	3.1 ± 6.0	0.0–27.3
Mn	51.2 ± 126.6	0.0–431.3	58.9 ± 120.4	0.0–405.1	49.9 ± 116.2	0.0–394.4
Fe	132.3 ± 192.4	0.0–829.5	174.7 ± 180.4	7.2–865.9	154.0 ± 160.1	0.0–478.9
Co	BDL	BDL	2.3 ± 8.2	0.0–42.7	2.2 ± 10.4	0.0–57.5
Ni	76.9 ± 150.3	0.0–484.7	85.8 ± 147.7	0.0–505.7	78.4 ± 134.7	0.0–465.1
Cu	2.4 ± 3.0	0.0–11.3	6.2 ± 6.2	0.1–24.6	5.2 ± 8.7	0.0–47.2
Zn	28.1 ± 39.5	0.0–144.9	35.4 ± 36.7	0.0–106.9	62.1 ± 97.8	0.0–395.0
As	8.8 ± 15.8	0.0–46.1	8.7 ± 16.3	0.0–54.1	9.6 ± 19.3	0.0–68.2
Se	4.6 ± 4.3	0–8.5	4.6 ± 4.3	0.0–8.5	4.6 ± 4.3	0.0–8.5
Cd	BDL	BDL	1.2 ± 3.4	0.0–16.8	1.9 ± 4.4	0.0–17.0
Ba	15.5 ± 24.4	0.0–108.7	24.3 ± 31.1	0.0–146.3	29.3 ± 48.8	0.0–239.5
Ce	BDL	BDL	0.6 ± 0.4	0.1–1.8	0.6 ± 0.5	0.0–2.3
Pt	BDL	BDL	BDL	BDL	BDL	BDL
Pb	3.6 ± 5.0	0.0–17.4	7.0 ± 13.9	0.0–66.2	10.8 ± 22.1	0.0–109.6
(**b**)						
	PM_{10}, Carbonaceous Species, and Ions ($\mu g/m^3$)					
PM	21.9 ± 8.7	3.4–36.9	21.0 ± 7.0	5.8–33.2	22.6 ± 7.9	6.2–36.9
OC	2.7 ± 0.9	1.2–4.9	4.8 ± 1.8	2.6–10.5	2.9 ± 1.0	1.0–5.3
EC	0.3 ± 0.4	0.0–1.4	1.2 ± 1.0	0.0–3.8	0.7 ± 0.3	0.2–1.4
POC	1.2 ± 0.4	0.5–2.1	2.0 ± 1.6	0.4–6.1	1.3 ± 0.6	0.3–2.6

Table 1. *Cont.*

	Ari		Din Daeng		Bangna	
	Mean ± Stdv	**Range**	**Mean ± Stdv**	**Mean ± Stdv**	**Range**	**Mean ± Stdv**
SOC	1.5 ± 0.8	0.0–3.2	2.9 ± 1.2	0.0–6.2	1.7 ± 0.8	0.0–3.8
Na^+	0.3 ± 0.3	0.0–0.8	0.3 ± 0.3	0.0–1.9	0.3 ± 0.3	0.0–0.8
NH_4^+	BDL	BDL	BDL	BDL	BDL	BDL
K^+	0.1 ± 0.1	0.0–0.5	0.1 ± 0.2	0.0–0.6	0.1 ± 0.2	0.0–0.6
Mg^{2+}	0.1 ± 0.1	0.0–0.2	0.1 ± 0.1	0.0–0.2	0.1 ± 0.1	0.0–0.2
Ca^{2+}	0.3 ± 0.4	0.0–1.1	0.3 ± 0.4	0.0–1.3	0.2 ± 0.3	0.0–0.8
NO_3^-	0.3 ± 0.2	0.0–1.0	0.4 ± 0.2	0.0–0.9	0.4 ± 0.2	0.1–0.9
SO_4^{2-}	1.1 ± 0.9	0.1–3.3	1.0 ± 0.8	0.0–3.2	1.1 ± 0.9	0.0–3.4
Cl^-	0.4 ± 0.2	0.1–1.1	0.4 ± 0.3	0.1–1.3	0.4 ± 0.2	0.1–0.9
	Metals (ng/m^3)					
Na	193.2 ± 404.0	0.0–1438.6	475.4 ± 844.4	0.0–3315.4	634.0 ± 1476.4	0.0–7709.7
Mg	337.5 ± 425.7	0.0–1373.8	354.6 ± 335.5	7.5–1290.3	366.4 ± 386.4	0.0–1262.4
Al	264.3 ± 288.1	0.0–876.9	462.9 ± 778.9	0.0–3593.7	549.4 ± 1082.6	0.0–5441.3
K	70.9 ± 167.2	0.0–643.2	119.4 ± 221.5	0.0–977.2	158.3 ± 379.6	0.0–1884.7
Ca	514.2 ± 798.6	0.0–3048.4	791.6 ± 576.3	0.0–1893.3	482.5 ± 743.5	0.0–2555.2
Sc	22.1 ± 30.2	0.0–107.7	23.1 ± 30.9	0.0–101.9	24.6 ± 33.4	0.0–118.1
Ti	26.4 ± 37.9	0.0–124.3	34.5 ± 41.8	0.0–160.1	27.6 ± 35.8	0.0–106.8
V	BDL	BDL	BDL	BDL	BDL	BDL
Cr	1.3 ± 2.4	0.0–11.8	3.3 ± 6.8	0.0–36.4	1.6 ± 4.3	0.0–22.5
Mn	33.5 ± 66.9	0.0–210.3	27.3 ± 52.8	0.0–165.6	26.6 ± 58.0	0.0–183.5
Fe	325.8 ± 270.4	0.0–1021.5	502.4 ± 356.3	115.1–1586.2	345.3 ± 243.4	20.4–819.9
Co	1.1 ± 6.1	0.0–33.7	0.5 ± 2.7	0.0–15.0	BDL	BDL
Ni	39.9 ± 72.8	0–242.6	40.8 ± 69.3	0.0–225.8	38.8 ± 66.6	0.0–234.4
Cu	1.4 ± 2.2	0.0–10.0	5.7 ± 8.3	0.0–42.5	2.0 ± 2.4	0.0–7.6
Zn	47.7 ± 187.7	0.0–1037.9	18.8 ± 31.0	0.0–119.6	20.3 ± 33.8	0.0–139.8
As	4.6 ± 9.5	0.0–30.0	3.6 ± 8.1	0.0–30.1	3.9 ± 8.3	0.0–31.7
Se	BDL	BDL	BDL	BDL	BDL	BDL
Cd	BDL	BDL	BDL	BDL	BDL	BDL
Ba	7.8 ± 18.2	0.0–93.5	17.9 ± 24.9	0.0–106.4	12.0 ± 25.2	0.0–115.8
Ce	0.3 ± 0.3	0.0–1.0	0.4 ± 0.5	0.0–2.4	0.4 ± 0.5	0.0–2.2
Pt	BDL	BDL	BDL	BDL	BDL	BDL
Pb	2.7 ± 9.9	0.0–54.7	2.7 ± 6.1	0.0–29.5	3.7 ± 7.7	0.0–35.0

BDL: Below detection limit.

Compared to Ari and Bangna, the average concentration of $PM_{2.5}$ and PM_{10} in Din Daeng was higher, since the Din Daeng site is close to an industrial zone. Furthermore, $PM_{2.5}$ and PM_{10} mass concentrations exhibited similar variations at all sampling sites. The average concentration of $PM_{2.5}$ measured in Bangkok (23.6 $\mu g/m^3$) was slightly lower than all sites of the current study, whereas the PM_{10} (53.4 $\mu g/m^3$) measured in the previous study was higher than in the current study [30]. In this region, the mass of PM may have been influenced by biomass combustion, industrial emissions, heavy traffic, the open burning of agricultural residues, and construction and demolition [31,32]. The concentration of $PM_{2.5}$ in the current study is reported to be higher than the permissible limit set by WHO, and can cause serious health problems. Therefore, this study highly recommends that in urban areas, the aerosol study should focus more on particles of 2.5 µm or less. As shown in Table 2, according to Spearman's rank correlation, the meteorological parameters, such as relative humidity, show strong correlation with $PM_{2.5}$ at Ari and Din Daeng, and a moderate correlation at Bangna. Likewise, windspeed shows a negative correlation with the mass concentration of $PM_{2.5}$ at Ari and Din Daeng. In contrast, there is no correlation between weather conditions and the mass of PM_{10}.

3.1.2. Carbonaceous Species

Table 1a,b shows the concentration of OC and EC in $PM_{2.5}$ and PM_{10} samples. At all sampling sites, the carbonaceous species were dominant in both $PM_{2.5}$ and PM_{10}. As

shown in Figure 3, OC is more dominant than EC at all sampling sites. Higher OC was observed at Din Daeng in both $PM_{2.5}$ (38.0 μg/m^3) and PM_{10} (22.3 μg/m^3), followed by Ari: $PM_{2.5}$ (28.2 μg/m^3) and Bangna: PM_{10} (11.2 μg/m^3). EC exhibited similar variation characteristics at all sites for $PM_{2.5}$ and PM_{10}. These results are similar to previous studies conducted in various cities of China [33,34]. The strong correlation between OC and EC suggests that both are emitted from the same sources. As shown in Figure 4, a strong correlation between OC and EC is observed in both $PM_{2.5}$ and PM_{10} at Ari and Din Daeng. At the same time, there is a moderate/weak correlation between OC and EC of $PM_{2.5}$ and PM_{10} at Bangna. The weak OC and EC correlations indicate the secondary aerosol formation under favourable conditions for the gas-to-particle conversion of volatile organic compounds (VOCs) through photochemical reactions [35]. Possible sources of the high concentrations of OC and EC include increased coal combustion, biomass burning, and unfavorable meteorological conditions [18]. OC consists of both primary organic carbon (POC) and secondary organic carbon (SOC). The contribution of SOC to OC in $PM_{2.5}$ was 69.5% (Ari), 78.1% (Din Daeng), and 75.7% (Bangna). In contrast, the SOC contribution to OC in PM_{10} was 57.0% (Ari), 58.3% (Din Daeng), and 63.3% (Bangna). Due to the role of high photochemical activity in its formation, SOC significantly contributes to OC [36].

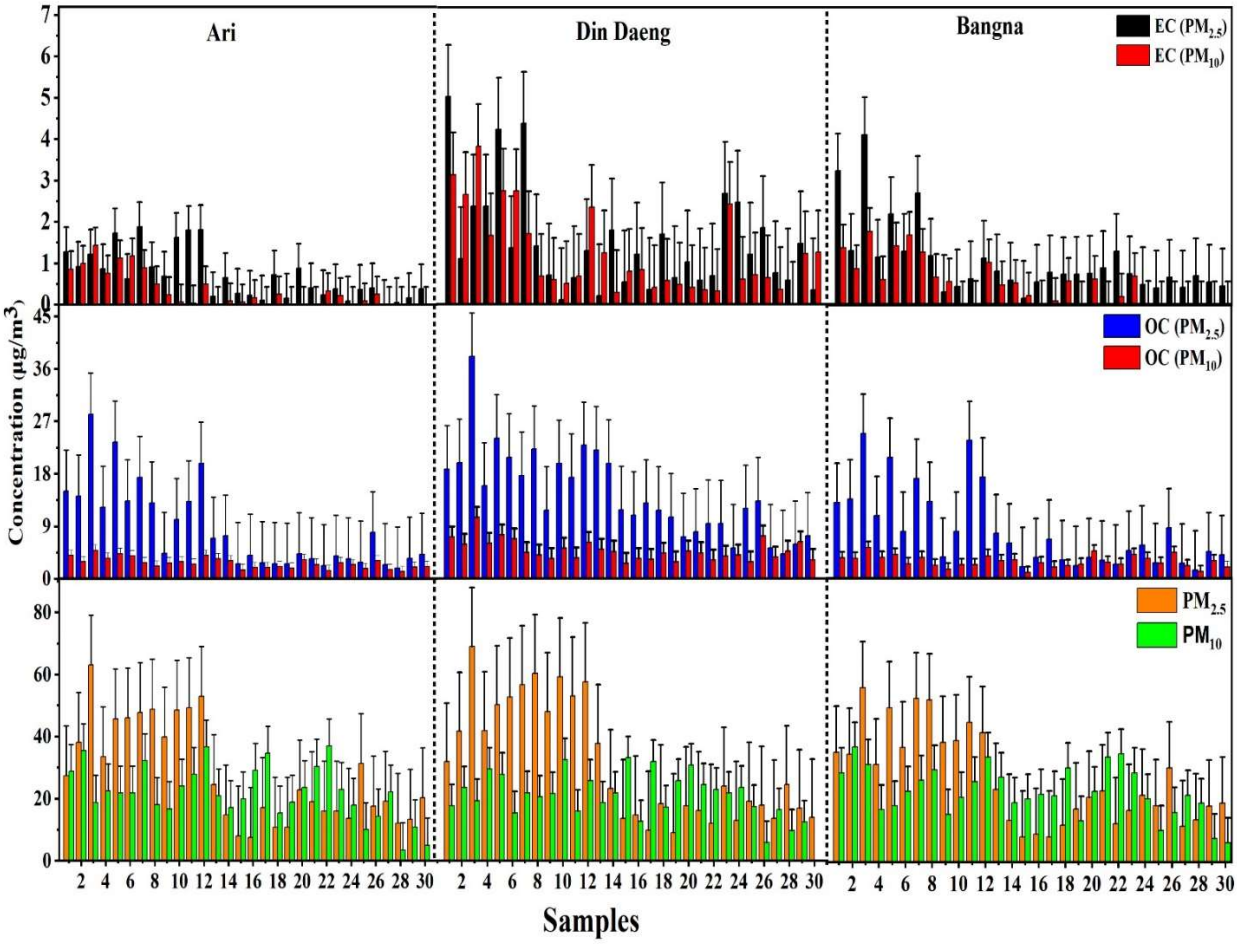

Figure 3. PM and its carbonaceous species at Ari, Din Daeng, and Bangna, Bangkok, Thailand.

Table 2. Spearman's rank correlation between $PM_{2.5}$, PM_{10}, and meteorological parameters.

	Ari		Din Daeng		Bangna	
	$PM_{2.5}$	**PM_{10}**	**$PM_{2.5}$**	**PM_{10}**	**$PM_{2.5}$**	**PM_{10}**
Temperature	0.10	−0.02	0.15	0.01	0.21	−0.16
Wind Speed	−0.44 *	0.31	−0.49 **	0.26	−0.36	0.29
Relative Humidity	0.48 **	−0.39 *	0.69 **	−0.31	0.36 *	−0.24

Level of significance: * $p < 0.05$; ** $p < 0.01$.

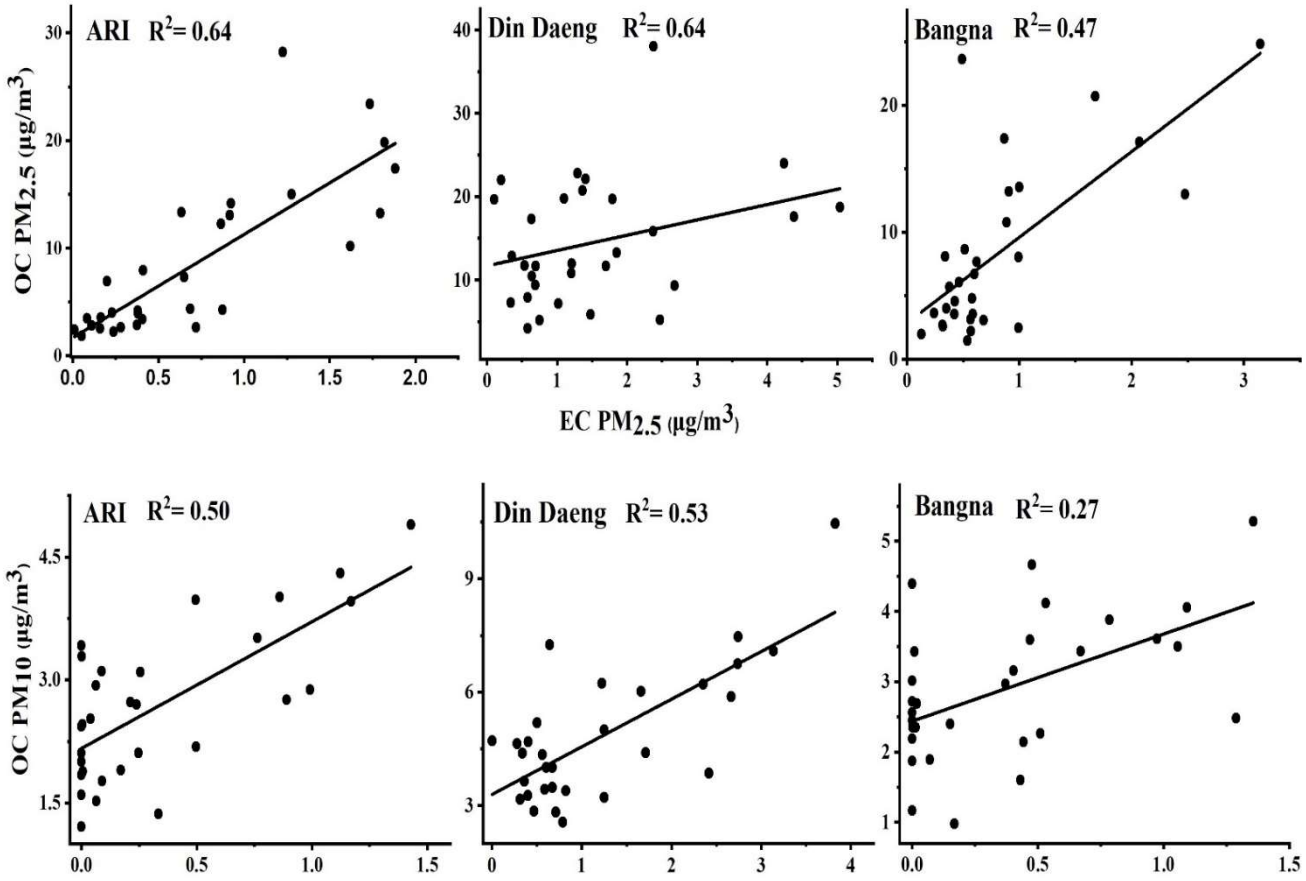

Figure 4. Scatter plots for OC and EC: $PM_{2.5}$ and PM_{10} for Ari, Din Daeng, and Bangna, Bangkok, Thailand.

3.1.3. Chemical Species

In Table 1a,b, the mean concentrations of water-soluble inorganic species (WSIS) in fine and coarse particles at Ari, Din Daeng, and Bangna are shown. At Ari, the WSIS concentrations in $PM_{2.5}$ were reported to be in descending order of $Cl^- > NH_4^+ > K^+ > Na^+ > Ca^{2+} > SO_4^{2-} > NO_3^- > Mg^{2+}$; the trend in the concentration at Din Daeng and Bangna followed the order of Ari. As for PM_{10}, the concentration of WSIS at Ari, Din Daeng, and Bangna was as follows: $SO_4^{2-} > Cl^- > Ca^{2+} > NO_3^- > Na^+ > K^+ > Mg^{2+} > NH_4^+$. At all three sites, the most abundant cations with high concentrations were ammonium (NH_4^+), potassium (K^+), calcium (Ca^{2+}), sodium (Na^+), and magnesium (Mg^{2+}), whereas the anions with the highest concentrations were chloride (Cl^-), sulfate (SO_4^{2-}), and nitrate (NO_3^-). Of the anions, Cl^-, and in cations, Ca^{2+}, was found dominant at all sites. Crustal inputs from the exposed surface soil or re-suspension of soil dust can contribute to the higher concentration of Ca^{2+}. At all sites, the higher concentration of Ca^{2+} in $PM_{2.5}$ and PM_{10} can also be attributed to the drier weather conditions [37]. During the secondary gas phase, SO_4^{2-} and NO_3^- are mainly formed [38]. NOx is a well-known precursor of NO_3^-, mainly released by vehicle exhaust (mobile sources). However, SO_4^{2-} is emitted mainly by coal-fired processes (stationary sources). The higher contributions of SO_4^{2-} and NO_3^- among anions to the mass of PM at all sites can be attributed to vehicular and industrial emissions [39]. The formation of sulfate-rich particles is mainly due to a change in equilibrium between the particle and gaseous phases caused by lower temperatures and higher humidity [40]. The HNO_3 and NH_3 gas-phase reaction formed NO_3^- ions in $PM_{2.5}$ [41]. In PM_{10}, sea salt or soil dust particles react with HNO_3 gas to form NO_3^- [42]. The major source of ammonium salt is the formation of secondary particles by aqueous or gas-phase reactions of NH_3 with H_2SO_4, HNO_3, and HCl. Potassium in $PM_{2.5}$ is derived

mainly from biomass burning, crop residues, and coal combustion [43]. Minerals of crustal origin are the major sources of potassium in the coarse mode [44]. Potential sources of Cl^- include the burning of waste plastic as a fuel at the residential and industrial levels, and its open burning [45]. Incinerators and power plants also contributed to Cl^- emissions [46]. Na^+ and Cl^- ions also contributed to the mass of aerosol due to the long-range transport of marine dust [44].

In Table 1a,b, the mean concentration of metal elements in $PM_{2.5}$ and PM_{10} at all sites are listed. The metal contribution to the mass of $PM_{2.5}$ at Ari, Din Daeng, and Bangna was 29.0%, 23.2%, and 35.1%, respectively, whereas for PM_{10}, the metal contribution at all sampling sites was 21.1% (Ari), 20.0% (Din Daeng), and 26.2% (Bangna). A significant contribution of metals to the mass of $PM_{2.5}$ and PM_{10} was observed at all sampling sites. Anthropogenic emission sources, such as biomass burning, coal combustion for barbecues on streets and roadsides, and industrial emissions, are possible sources of high contributions of metals to the mass of PM. In addition, unfavorable climatic conditions, such as temperature inversions and low wind speeds at all sampling sites, inhibit the dispersion of pollutants. K is used as a marker of biomass and wood burning in several source apportionment studies conducted in various regions [47]. Therefore, the high concentration of K is due to biomass burning and coal combustion in current study. Gasoline additives, brake pads, and road dust re-suspension contribute to the high concentration of Pb that can cause human health problems [48]. Fuel combustion in cars, buses, trucks, motorcycles, rickshaws, etc., and tyre wear are the possible sources of the higher zinc (Zn) concentration at all sites [49].

3.2. Health Risk Assessment

The serious carcinogenic and non-carcinogenic toxicity of $PM_{2.5}$- and PM_{10}-bound metals in humans depends on the frequency, exposure duration, and concentration of metals. A health risk assessment of heavy metals for adults and children via inhalation pathways was determined. Table 3 presents the hazard quotient (HQ) and cancer risk (CR) values of $PM_{2.5}$ and PM_{10} for both adults and children. At all sites, the non-carcinogenic risks of As, Cd, Cr, Mn, and Ni of $PM_{2.5}$ and PM_{10} were below the safe level (HQ = 1) for children. In contrast, at Ari and Din Daeng, the HQ values of Ni and Mn of $PM_{2.5}$ for adults exceeded the safe level. Moreover, the HQ value of Ni for adults in $PM_{2.5}$ at Bangna also exceeded the safe level, indicating that the inhalation of these metals can cause non-carcinogenic health effects. NI and Mn posed no non-carcinogenic risks to both adults and children in Nanjing, China [50], and Mexico [51]. As illustrated in Table 3, the non-carcinogenic risks of $PM_{2.5}$ and PM_{10} for adults and children were in decreasing order: Cd > Cr > As > Mn > Ni at Ari, Din Daeng, and Bangna. Normally, coarse particles tend to deposit and may be expelled in the nasal-pharyngeal region. In contrast, $PM_{2.5}$ can enter the respiratory tract, penetrate deep into the lungs, and cause serious health problems. The non-carcinogenic risk posed by the toxic elements of $PM_{2.5}$ for adults was significantly higher in Bangkok.

The health risk assessment of heavy metals indicated that the Cr of $PM_{2.5}$ and PM_{10} pose a carcinogenic risk to adults at Bangna and Din Daeng. Similar results for the carcinogenic risk value of Cr exceeded the permissible limits obtained in India [52] and Tianjin, China [53]. In contrast, at all sites, the carcinogenic risk values, f, of Cd, Ni, As, and Pb were below the safe level for both adults and children. The total carcinogenic risk exceeded the permissible limit for adults at all sites, exposing adults in Bangkok to high carcinogenic risk. The non-carcinogenic risk posed by Ni and Mn and the carcinogenic risk by Cr to adults via inhalation are the most serious threats to the residents of Bangkok.

Table 3. Carcinogenic and non-carcinogenic risk of heavy metals via inhalation exposure of $PM_{2.5}$ and PM_{10} at Ari, Din Daeng, and Bangna, Bangkok, Thailand.

$PM_{2.5}$	Carcinogenic (CR)		Non-Carcinogenic (HQ)		PM_{10}	Carcinogenic (CR)		Non-Carcinogenic (HQ)	
Ari	**Children**	**Adult**	**Children**	**Adult**		**Children**	**Adult**	**Children**	**Adult**
As	3.26×10^{-6}	1.63×10^{-5}	1.89×10^{-1}	5.66×10^{-1}		1.68×10^{-6}	8.42×10^{-6}	8.23×10^{-2}	2.47×10^{-1}
Cd	1.25×10^{-7}	6.23×10^{-7}	2.58×10^{-2}	7.75×10^{-2}		5.40×10^{-8}	2.70×10^{-7}	1.92×10^{-2}	5.75×10^{-2}
Cr	1.82×10^{-5}	9.11×10^{-5}	8.29×10^{-2}	2.49×10^{-2}		8.86×10^{-6}	4.43×10^{-5}	5.25×10^{-2}	1.58×10^{-2}
Pb	2.46×10^{-6}	1.23×10^{-7}	NA	NA		1.81×10^{-8}	9.35×10^{-8}	NA	NA
Ni	1.58×10^{-6}	7.91×10^{-6}	4.91×10^{-1}	1.47×10^{0}		8.21×10^{-6}	4.10×10^{-6}	2.48×10^{-1}	7.44×10^{-1}
Mn	NA	NA	3.27×10^{-1}	1.02×10^{0}		NA	NA	1.70×10^{-1}	5.09×10^{-1}
Total	2.32×10^{-5}	1.16×10^{-4}	1.04×10^{0}	3.16×10^{0}		1.14×10^{-5}	5.72×10^{-5}	5.25×10^{-1}	1.57×10^{0}
Din Daeng									
As	3.21×10^{-6}	1.60×10^{-5}	1.86×10^{-1}	5.57×10^{-1}		1.31×10^{-6}	6.55×10^{-6}	7.58×10^{-2}	2.27×10^{-1}
Cd	1.85×10^{-7}	9.24×10^{-7}	3.83×10^{-2}	1.15×10^{-1}		9.00×10^{-8}	4.50×10^{-7}	1.86×10^{-2}	5.59×10^{-2}
Cr	1.37×10^{-5}	6.83×10^{-5}	6.22×10^{-2}	1.86×10^{-2}		2.29×10^{-5}	1.15×10^{-4}	1.04×10^{-2}	1.58×10^{-2}
Pb	4.82×10^{-8}	2.41×10^{-7}	NA	NA		1.85×10^{-8}	9.23×10^{-8}	NA	NA
Ni	1.77×10^{-6}	8.83×10^{-6}	5.49×10^{-1}	1.65×10^{0}		8.38×10^{-7}	4.19×10^{-6}	2.61×10^{-1}	7.44×10^{-1}
Mn	NA	NA	3.77×10^{-1}	1.13×10^{0}		NA	NA	1.75×10^{-1}	5.09×10^{-1}
Total	1.89×10^{-5}	9.44×10^{-5}	1.16×10^{0}	3.47×10^{0}		2.52×10^{-5}	1.26×10^{-4}	5.40×10^{-1}	1.57×10^{0}
Bangna									
As	3.52×10^{-6}	1.77×10^{-5}	2.05×10^{-1}	6.14×10^{-1}		1.42×10^{-6}	7.11×10^{-6}	8.23×10^{-2}	2.47×10^{-1}
Cd	9.10×10^{-8}	1.46×10^{-6}	6.03×10^{-2}	1.81×10^{-1}		9.26×10^{-8}	4.63×10^{-7}	1.92×10^{-2}	5.75×10^{-2}
Cr	3.30×10^{-5}	1.09×10^{-4}	9.88×10^{-2}	2.96×10^{-2}		1.16×10^{-5}	5.78×10^{-5}	5.25×10^{-2}	1.58×10^{-2}
Pb	9.36×10^{-9}	3.70×10^{-7}	NA	NA		2.51×10^{-8}	1.25×10^{-7}	NA	NA
Ni	2.93×10^{-6}	8.07×10^{-6}	5.01×10^{-1}	1.50×10^{0}		7.98×10^{-7}	3.99×10^{-6}	2.48×10^{-1}	7.44×10^{-1}
Mn	NA	NA	3.19×10^{-1}	9.57×10^{-1}		NA	NA	1.70×10^{-1}	5.09×10^{-1}
Total	2.72×10^{-5}	1.36×10^{-4}	1.10×10^{0}	3.29×10^{0}		1.39×10^{-5}	6.94×10^{-5}	5.25×10^{-1}	1.57×10^{0}

CR: carcinogenic risk; HQ: hazard quotient; NA: not available.

3.3. Source Apportionment Using Principal Component Analysis (PCA)

PCA was used to identify sources associated with carbonaceous species, inorganic ions, and major elements in $PM_{2.5}$ and PM_{10}. The PCA with the varimax rotational factor analysis method was conducted using the Statistical Package for Social Sciences (SPSS v20.0) to identify the sources of $PM_{2.5}$ and PM_{10} at Ari, Din Daeng, and Bangna. Factor 1 contributes 35.6%, 26.8%, and 31.8% to the total variance at Ari, Din Daeng, and Bangna, respectively. Factor 1 of $PM_{2.5}$ was interpreted as industrial emissions and dust/crustal re-suspension at Ari having high Mg^{2+}, Ca^{2+}, Al, Ti, Cr, Mn, As, and Ni loadings, as shown in Table 4a. At Din Daeng, factor 1 represents industrial emissions and dust re-suspension with high loadings of Mg^{2+}, Ca^{2+}, Ti, Mn, Ni, and As. In contrast, at Bangna, factor 1 is highly loaded with OC, EC, NH_4^+, K^+, NO_3^-, SO_4^{2-}, Cl^-, and Fe, which represent primary combustion sources, including vehicle emissions, biomass burning, coal combustion, and secondary aerosol formation. Factor 2 contributed 20.8% (Ari), 18.7% (Din Daeng), and 25.2% (Bangna) of the total variance. Factor 2 of $PM_{2.5}$ at Ari, Din Daeng, and Bangna represents secondary aerosol formation plus sea salt, primary combustion sources (biomass burning and vehicle emission), and industrial emissions. High loadings of Na^+, NH_4^+, NO_3^-, SO_4^{2-}, Cl^-, and Fe are found at Ari. At Din Daeng, high loadings of OC, EC, NH_4^+, Cl^-, K^+, and Fe are found. Ti, As, Ni, and Mn are highly loaded at Bangna.

At Ari, factor 3 is considered the primary combustion source (vehicle emission and biomass burning), contributing 16.0% to the total variance, and is highly loaded with OC, EC, and K^+. Factor 3 contributes 17.7% of the variance in Din Daeng, loaded with Na^+, NO_3^-, and SO_4^{2-}. Therefore, it is categorized as sea salt and secondary aerosol formation. The third factor in Bangna is rich in Na^+ and moderate in Al, indicating a sea salt source, contributing 12.0% of the variance. The use of some markers is perplexing and can be affected by various sources, specifically K^+ from wood and biomass burning, Cl^- from sea salt and coal combustion, and Mg from crustal emissions. The presence of NO_3^- indicates the probability of a marine origin through HNO_3 condensation [54,55]. Factor 4 at Ari is rich in Cu and Zn, accounting for 9.2% of the variance. The traffic source profile is also associated with Cu and Zn [56]. As a result, factor 4 at Ari is considered traffic/road dust. Factor 4, rich in Al and Ti at Din Daeng, contributed 12.7% of the variance. Al, Ti,

and other trace elements have been used in different studies as a source of resuspension of soil/crustal dust [57]. As a result, at Din Daeng, factor 4 is classified as crustal/dust re-suspension. At Bangna, factor 4 contributed 11.0% to the total variance and is rich in Cu and Zn, indicating traffic/road dust. According to PCA results, the dominant sources of $PM_{2.5}$ at Ari, Din Daeng, and Bangna are primary combustion sources (biomass burning, vehicle emissions, coal combustion), road dust re-suspension, secondary aerosol formation, and sea salt contribution.

Table 4. (**a**) Principal component analysis for selected species of $PM_{2.5}$ at Ari, Dindaeng, and Bangna, Bangkok, Thailand (**b**) Principal component analysis for selected species of PM_{10} at Ari, Dindaeng, and Bangna, Bangkok, Thailand.

(**a**)

	Ari				Din Daeng				Bangna			
Species	**F1**	**F2**	**F3**	**F4**	**F1**	**F2**	**F3**	**F4**	**F1**	**F2**	**F3**	**F4**
OC	−0.04	0.44	0.84	0.11	−0.02	0.94	0.13	0.12	0.76	0.12	−0.28	−0.24
EC	0.10	0.08	0.90	−0.15	−0.34	0.84	0.30	−0.75	0.78	−0.39	0.01	−0.11
Na^+	0.54	0.67	0.04	−0.08	0.22	0.06	0.90	0.06	0.41	0.36	0.93	−0.04
NH_4^+	0.05	0.91	0.08	0.06	0.02	0.73	0.41	0.19	0.92	−0.02	−0.19	−0.12
K^+	−0.08	0.58	0.71	0.22	−0.12	0.83	0.36	−0.02	0.76	−0.28	0.11	−0.12
Mg^{2+}	0.87	−0.01	−0.14	−0.26	0.89	−0.05	−0.22	−0.22	0.03	0.47	−0.68	0.20
Ca^{2+}	0.70	−0.31	−0.16	−0.36	0.67	−0.22	−0.21	−0.67	−0.34	0.55	−0.43	−0.08
NO_3^-	−0.35	0.71	0.27	0.13	−0.23	0.29	0.85	0.04	0.85	−0.13	0.26	0.14
SO_4^{2-}	−0.12	0.72	0.01	0.25	−0.16	0.44	0.75	0.39	0.86	−0.17	0.36	0.02
Cl^-	0.09	0.90	0.10	0.15	0.27	0.60	0.43	0.39	0.79	0.32	−0.08	0.05
Al	0.90	−0.16	−0.20	0.07	0.23	0.25	0.20	0.69	0.13	0.08	0.61	−0.06
Ti	0.98	0.02	−0.02	0.01	0.92	−0.06	0.13	0.57	−0.03	0.93	0.23	−0.07
Cr	0.93	0.30	−0.36	−0.10	0.46	−0.34	0.44	0.31	−0.44	0.33	0.44	0.48
Mn	0.96	0.01	0.12	−0.01	0.95	−0.04	0.17	0.15	−0.13	0.94	−0.10	−0.15
Fe	−0.40	0.71	0.45	−0.01	−0.11	0.62	0.42	−0.17	0.88	−0.19	0.40	−0.03
Ni	0.97	0.04	0.05	−0.06	0.89	−0.04	0.15	0.17	−0.03	0.96	0.01	−0.09
Cu	−0.10	0.32	0.09	0.70	−0.04	0.36	0.50	0.07	−0.23	−0.25	0.03	0.88
Zn	−0.06	−0.05	0.03	0.92	0.18	0.13	0.07	0.67	0.11	−0.21	−0.29	0.91
As	0.92	−0.06	0.04	0.02	0.94	−0.06	−0.04	0.16	−0.12	0.91	−0.20	−0.16
% of Variance	35.6	20.8	16.0	9.2	26.8	18.7	17.7	12.7	31.8	25.2	12.0	11.0
Cumulative %	35.6	56.4	72.4	81.6	26.8	45.5	63.1	75.8	31.8	57.1	69	79.9

(**b**)

	Ari				Din Daeng				Bangna			
Species	**F1**	**F2**	**F3**	**F4**	**F1**	**F2**	**F3**	**F4**	**F1**	**F2**	**F3**	**F4**
OC	−0.01	0.86	−0.22	0.01	0.89	0.37	−0.06	0.02	0.47	0.73	−0.03	−0.06
EC	−0.28	0.87	0.16	−0.11	0.9	0.30	−0.21	−0.04	0.57	0.75	−0.17	−0.22
Na^+	0.43	−0.07	0.78	0.02	−0.06	−0.07	0.93	0.09	0.12	−0.62	0.25	0.86
NH_4^+	−0.24	0.82	0.37	−0.12	0.85	0.30	0.02	−0.26	0.91	0.21	−0.22	0.08
K^+	−0.14	0.39	0.87	0.04	0.85	0.15	0.17	−0.35	0.86	−0.32	−0.17	0.08
Mg^{2+}	0.55	0.01	−0.29	−0.14	−0.06	0.01	0.66	0.42	−0.64	−0.24	0.38	0.50
Ca^{2+}	0.55	−0.31	−0.33	0.14	−0.49	−0.34	−0.12	0.70	−0.52	−0.03	0.29	−0.23
NO_3^-	0.84	−0.09	0.13	−0.05	−0.02	0.31	0.89	0.08	−0.31	0.05	0.35	0.84
SO_4^{2-}	0.62	0.30	−0.06	−0.58	0.40	0.11	0.65	0.17	0.47	0.22	0.23	0.78
Cl^-	0.40	0.65	0.26	0.33	0.56	0.61	0.45	0.02	0.44	0.37	0.13	0.79
Al	0.38	0.24	0.45	0.65	0.41	0.88	0.01	−0.01	0.69	0.04	0.15	0.08
Ti	0.84	0.20	0.22	0.42	0.24	0.79	0.35	0.37	0.35	0.19	0.76	0.39
Cr	0.06	0.15	−0.04	0.67	0.34	0.91	0.06	−0.08	0.08	0.83	0.07	0.39
Mn	0.91	−0.07	0.23	0.19	−0.01	0.29	0.32	0.89	−0.23	−0.05	0.93	0.18
Fe	0.01	0.91	0.11	0.22	0.86	0.40	0.12	0.03	0.66	0.64	−0.01	0.27
Ni	0.96	−0.10	−0.05	0.01	−0.11	0.11	0.58	0.76	−0.09	−0.18	0.90	0.27
Cu	−0.11	0.74	0.11	0.36	0.51	0.77	0.03	−0.19	0.02	0.79	−0.25	0.09
Zn	−0.11	0.08	0.94	0.11	0.19	0.91	0.04	0.03	−0.09	0.87	0.03	−0.04
As	0.92	−0.25	−0.04	0.06	−0.13	−0.11	0.16	0.95	−0.28	−0.12	0.93	0.04
% of Variance	29.9	23.9	16.2	9.5	27.2	25.6	17.9	17.6	23.8	21.4	20.0	17.1
Cumulative %	29.9	53.8	70	79.4	27.2	52.8	70.7	88.3	23.8	45.2	65.3	82.4

The species with a high loading in each factor is marked as underline.

As shown in Table 4b, the sources of PM_{10} at Ari, Din Daeng, and Bangna identified in the same way as $PM_{2.5}$. At Ari, Din Daeng, and Bangna, factor 1 is seen to contribute 29.9%, 27.3%, and 23.8% to the total variance. At Ari, factor 1 of PM_{10} was loaded with NO_3^-, SO_4^{2-}, Ti, Mn, Ni, and As, which are considered secondary aerosol formation and industrial emissions. Moreover, gaseous precursors such as NOx and SOx emitted from vehicles, fossil fuels, coal combustion, and industrial processes contribute to the formation of secondary nitrate and sulfate sources [58]. At Din Daeng, factor 1 is loaded with OC, EC, NH_4^+, K^+,

Cl^-, Cu, and Fe. Factor 1 represented primary combustion sources at Ding Daeng. At Bangna, the same factor is significantly loaded with NH_4^+, K^+, Al, and Fe, representing biomass burning. K^+ is used as a marker of biomass burning in various apportionment studies [59]. In several studies, the combination of NH_4^+ and K^+ has been used as a marker of combustion emissions [60]. At Ari, Din Daeng, and Bangna, factor 2 of PM_{10} contributed 23.9%, 25.6%, and 21.4% to the total variance, respectively. Factor 2 at Ari was loaded with OC, EC, NH_4^+, Cl^-, Fe, and Cu, and represented primary combustion sources such as vehicle emissions. At Din Daeng and Bangna, factor 2 represents crustal/road dust re-suspension and vehicle emissions, which are the possible sources of PM_{10}. At Din Daeng, factor 2 is loaded with Cl^-, Al, Ti, Cr, Cu, and Zn, whereas at Bangna, OC, EC, Cr, Cu, and Zn contributed highly to factor 2. Two-stroke engines emit zinc, which is used as a fuel additive to reduce tyre wear [56]. Factor 3 accounted for 16.2% (Ari), 17.9% (Din Daeng), and 20.0% (Bangna) of the total variance. Biomass combustion, sea salt/secondary aerosol formation, and industrial emissions are possible sources of PM_{10} at Ari, Din Daeng, and Bangna, represented by factor 3. At Ari, factor 3 is loaded with Na^+, K^+, and Zn, which represent biomass combustion. Factor 3 at Din Daeng is loaded with Na^+, Mg^{2+}, NO_3^-, SO_4^{2-}, and Ni, indicating sea salt/secondary aerosol formation, and at Bangna, factor 3 is loaded with Ti, Mn, Ni, and As, representing industrial emissions.

Factor 4 indicated crustal re-suspension, industrial emissions/sea salt, and secondary aerosol formation. At Ari, Din Daeng, and Bangna, the possible sources of PM_{10} in factor 4 account for 9.5%, 17.6%, and 17.1% of the total variance. According to the results of PCA, the major combustion sources, such as vehicle emissions, coal combustion, and biomass burning, and secondary aerosol formation, industrial emissions, sea salt contribution, and dust sources contributed to $PM_{2.5}$ and PM_{10} mass during the study period.

4. Conclusions

This paper investigated the $PM_{2.5}$ and PM_{10} mass concentrations at three sampling locations in Bangkok. At all sampling sites, the daily concentration of $PM_{2.5}$ exceeded the permissible limit of WHO guidelines. However, PM_{10} concentrations were found to be within the permissible limits. At Din Daeng, the average concentrations of $PM_{2.5}$ and PM_{10} were comparatively higher than at Ari and Bangna. The high $PM_{2.5}$ concentrations indicated serious fine particle pollution in Bangkok. At all sites, OC and EC were the dominant species reported in $PM_{2.5}$ and PM_{10}. At Din Daeng, the OC and EC concentrations were higher than at Ari and Bangna. The strong OC and EC correlation at Ari and Din Daeng indicated that they are emitted from the same sources. At Bangna, a weak correlation between OC and EC in both $PM_{2.5}$ and PM_{10} indicated secondary aerosol formation through photochemical reactions under favorable conditions. The SOC contribution to OC in $PM_{2.5}$ at Ari, Din Daeng, and Bangna was 69.5%, 78.1%, and 75.7%, respectively. Likewise, in PM_{10}, the SOC contribution to OC was 57.0% (Ari), 58.3% (Din Daeng), and 63.3% (Bangna). The contribution of SOC is due to the high photochemical activity.

A health risk assessment of heavy metals in $PM_{2.5}$ and PM_{10} through the inhalation pathway for adults and children was determined at Ari, Din Daeng, and Bangna. The non-carcinogenic risks of As, Cd, Cr, Ni, and Mn of $PM_{2.5}$ and PM_{10} were below the permissible limits for children, except Mn and Ni of $PM_{2.5}$ for adults, which exceeded the safe level at Ari and Din Daeng. In contrast, the Ni value of $PM_{2.5}$ at Bangna for adults was also higher than the safe level. The non-carcinogenic risk of PM_{10} for both adults and children at all sites was below the safe level. The health risk assessment of heavy metals shows that Cr in $PM_{2.5}$ and PM_{10} poses a carcinogenic risk to adults at Bangna and Din Daeng. The total carcinogenic risk for adults exceeded the permissible limits, suggesting a carcinogenic risk in Bangkok. The possible sources of $PM_{2.5}$ and PM_{10} at Ari, Din Daeng, and Bangna are dust re-suspension, primary combustion sources such as biomass burning and vehicle emissions, coal combustion, secondary aerosol formation, and sea salt. Thus, the influence of marine and continental air masses contributed to the mass of $PM_{2.5}$ and PM_{10} during the sampling period in Bangkok. Legislators can use our findings to formulate efficient

strategies to mitigate the $PM_{2.5}$ and PM_{10} pollution in order to protect the health of the public in Bangkok.

Author Contributions: Conceptualization, S.P. and W.K.; methodology, W.R., P.M., R.S., A.K. and S.A.; software, M.A.; validation, W.R. and R.S.; formal analysis, T.M., W.R., P.M. and R.S.; investigation, R.S. and W.K.; resources, R.S.; data curation, W.K.; writing—original draft preparation, T.M., M.A. and S.P.; writing—review and editing, S.P. and M.A.; visualization, K.S.; supervision, W.K.; project administration, W.K.; funding acquisition, S.P. and W.K. All authors have read and agreed to the published version of the manuscript.

Funding: This research was funded by [National Research Council of Thailand] grant number [NR. (Wor.) (PorSor)/395/2563]. The APC was funded by Research Affairs and Faculty of Engineering, Chulalongkorn University Bangkok, Thailand.

Institutional Review Board Statement: Not applicable.

Informed Consent Statement: This research does not use "human or animal subjects". Instead, it is based on observing atmospheric aerosols and meteorological parameters, which do not need ethical approval. This research does not involve any "human participant", so informed consent is not required. The consent to publish has been received from all the authors involved in this research.

Data Availability Statement: The original contributions are presented in the study; further inquiries can be directed to the corresponding authors. Data used in the present study can be obtained by contacting sirima.p@chula.ac.th.

Acknowledgments: The first author is grateful to the second century fund (C2F), Chulalongkorn University Bangkok, Thailand, for a postdoctoral fellowship. This research work is supported and was provided funding by the Thailand Graduate Institute of Science and Technology (SCA-CO-2564-14608-TH); and C2F, Chulalongkorn University, Bangkok, Thailand. Sirima Panyametheekul was awarded the flagship Thailand Citizen RDI X-Prize Quadruple Helix of National Research Council of Thailand in 2020 (NR. (Wor.) (PorSor)/395/2563).

Conflicts of Interest: The authors declare no conflict of interest.

References

1. Harrison, R.M.; Bousiotis, D.; Mohorjy, A.; Alkhalaf, A.; Shamy, M.; Alghamdi, M.; Khoder, M.; Costa, M. Health risk associated with airborne particulate matter and its components in Jeddah, Saudi Arabia. *Sci. Total Environ.* **2017**, *590*, 531–539. [CrossRef] [PubMed]
2. Crobeddu, B.; Aragao-Santiago, L.; Bui, L.C.; Boland, S.; Baeza-Squiban, A. Oxidative potential of particulate matter 2.5 as predictive indicator of cellular stress. *Environ. Pollut.* **2017**, *230*, 125–133. [CrossRef] [PubMed]
3. Gurjar, B.R.; Jain, A.; Sharma, A.; Agarwal, A.; Gupta, P.; Nagpure, A.S.; Lelieveld, J. Human health risks in megacities due to air pollution. *Atmos. Environ.* **2010**, *44*, 4606–4613. [CrossRef]
4. Ma, Y.; Weber, R.J.; Lee, Y.N.; Orsini, D.A.; Maxwell-Meier, K.; Thornton, D.C.; Bandy, A.R.; Clarke, A.D.; Blake, D.R.; Sachse, G.W.; et al. Characteristics and influence of biosmoke on the fine-particle ionic composition measured in Asian outflow during the transport and chemical evolution over the Pacific (TRACE-P) experiment. *J. Geophys. Res.* **2003**, *108*, 8816. [CrossRef]
5. Terzi, E.; Argyropoulos, G.; Bougatioti, A.; Mihalopoulos, N.; Nikolaou, K.; Samara, C. Chemical composition and mass closure of ambient PM_{10} at urban sites. *Atmos. Environ.* **2010**, *44*, 2231–2239. [CrossRef]
6. Viana, M.; Maenhaut, W.; Chi, X.; Querol, X.; Alastuey, A. Comparative chemical mass closure of fine and coarse aerosols at two sites in south and west Europe: Implications for EU air pollution policies. *Atmos. Environ.* **2007**, *41*, 315–326. [CrossRef]
7. Wang, Q.Q.; Huang, X.H.H.; Zhang, T.; Zhang, Q.; Feng, Y.; Yuan, Z.; Wu, D.; Lau, A.K.H.; Yu, J.Z. Organic tracer-based source analysis of $PM_{2.5}$ organic and elemental carbon: A case study at Dongguan in the Pearl River Delta, China. *Atmos. Environ.* **2015**, *118*, 164–175. [CrossRef]
8. Yang, F.; Huang, L.; Sharma, S.; Brook, J.R.; Zhang, W.; Li, S.M.; Tan, J. Two-year observations of fine carbonaceous particles in variable sampling intervals. *Atmos. Environ.* **2011**, *45*, 2418–2426. [CrossRef]
9. Tsai, Y.I.; Kuo, S.C. PM2.5 Aerosol water content and chemical composition in a metropolitan and a coastal area in southern Taiwan. *Atmos. Environ.* **2005**, *39*, 4827–4839. [CrossRef]
10. Greene, N.A.; Morris, V.R. Assessment of public health risks associated with atmospheric exposure to $PM_{2.5}$ in Washington, DC, USA. *Int. J. Environ. Res. Public Health* **2006**, *3*, 86–97. [CrossRef]
11. Kim, K.H.; Kabir, E.; Kabir, S. A review on the human health impact of airborne particulate matter. *Environ. Int.* **2015**, *74*, 136–143. [CrossRef] [PubMed]

12. Cao, J.J.; Xu, H.M.; Xu, Q.; Chen, B.H.; Kan, H.D. Fine particulate matter constituents and cardiopulmonary mortality in a heavily polluted Chinese city. Environ. *Health Perspect.* **2012**, *120*, 373–378. [CrossRef] [PubMed]
13. Lee, B.K.; Hieu, N.T. Seasonal variation and sources of heavy metals in atmospheric aerosols in a residential area of Ulsan, Korea. *Aerosol Air Qual. Res.* **2011**, *11*, 679–688.
14. Feng, B.; Li, L.; Xu, H.; Wang, T.; Wu, R.; Chen, J.; Zhang, Y.; Liu, S.; Ho, S.S.H.; Cao, J.; et al. $PM_{2.5}$-bound polycyclic aromatic hydrocarbons (PAHs) in Beijing: Seasonal variations, sources, and risk assessment. *J. Environ. Sci.* **2019**, *77*, 11–19. [CrossRef] [PubMed]
15. Karlsson, H.L.; Gustafsson, J.; Cronholm, P.; Möller, L. Size-dependent toxicity of metal oxide particles, a comparison between nano- and micrometer size. *Toxicol. Lett.* **2009**, *188*, 112–118. [CrossRef]
16. Chen, R.J.; Chen, B.H.; Kan, H.D. A health-based economic assessment of particulate air pollution in 113 Chinese cities. *Chin. J. Environ. Sci.* **2010**, *30*, 410–415.
17. Hou, Q.; An, X.Q.; Wang, Z.F.; Wang, Y.; Sun, Z.B. Assessment on health economic costs of particulate air pollution in Lanzhou during 2002–2009. *Chin. J. Environ. Sci.* **2011**, *31*, 1398–1402.
18. Ahmad, M.; Yu, Q.; Chen, J.; Cheng, S.; Qin, W.; Zhang, Y. Chemical characteristics, oxidative potential, and sources of $PM_{2.5}$ in wintertime in Lahore and Peshawar, Pakistan. *J. Environ. Sci.* **2021**, *102*, 148–158. [CrossRef]
19. Du, Y.; Gao, B.; Zhou, H.; Ju, X.; Hao, H.; Yin, S. Health risk assessment of heavy metals in road dusts in urban parks of Beijing, China. *Procedia Environ. Sci.* **2013**, *18*, 299–309. [CrossRef]
20. Castro, L.M.; Pio, C.A.; Harrison, R.M.; Smith, D.J.T. Carbonaceous aerosol in urban and rural European atmospheres: Estimation of secondary organic carbon concentrations. *Atmos. Environ.* **1999**, *33*, 2771–2781. [CrossRef]
21. Hopke, P.K. Recent developments in receptor modeling. *J. Chemother.* **2003**, *17*, 255–265. [CrossRef]
22. U.S. EPA. Risk assessment guidance for superfund (RAGS). In *Volume I: Human Health Evaluation Manual (Part F, Supplemental Guidance for Inhalation Risk Assessment)*; U.S. Environmental Protection Agency: Washington, DC, USA, 2009.
23. Li, Y.; Zhang, Z.; Liu, H.; Zhou, H.; Fan, Z.; Lin, M.; Wu, D.; Xia, B. Characteristics, sources, and health risk assessment of toxic heavy metals in $PM_{2.5}$ at a megacity of southwest China. *Environ. Geochem. Health* **2016**, *38*, 353–362. [CrossRef]
24. Li, H.; Qian, X.; Hu, W.; Wang, Y.; Gao, H. Chemical speciation and human health risk of trace metals in urban street dust from a metropolitan city, Nanjing, SE China. *Sci. Total Environ.* **2013**, *456*, 212–221. [CrossRef] [PubMed]
25. Ferreira-Baptista, L.; De Miguel, E. Geochemistry and risk assessment of street dust in Luanda, Angola: A tropical urban environment. *Atmos. Environ.* **2005**, *39*, 4501–4512. [CrossRef]
26. Tian, H.Z.; Wang, Y.; Xue, Z.G.; Cheng, K.; Qu, Y.P.; Chai, F.H.; Hao, J.M. Trend and characteristics of atmospheric emissions of Hg, As and Se from coal combustion in China, 1980–2007. *Atmos. Chem. Phys.* **2010**, *10*, 11905–11919. [CrossRef]
27. Thongyen, T.; Limpaseni, W.; Preuksasit, T.; Otani, Y.; Furuuchi, M. Nanoparticles concentrations in Bangkok ambient air. In Proceedings of the 2010 Annual Meeting of Japan Society of Civil Engineers, Chubu branch, Kanazawa, Japan, 7 September 2010; Kanazawa Institute of Technology: Ishikawa, Japan, 2010; Volume VII-18, pp. 577–588.
28. Wimolwattanapun, W.; Hopke, P.K.; Pongkiatkul, P. Source apportionment and potential source location of $PM_{2.5}$ and $PM_{2.5\text{-}10}$ at residential sites in Metropolitan Bangkok. *Atmos. Pollut. Res.* **2011**, *2*, 172–181. [CrossRef]
29. Sakunkoo, P.; Thonglua, T.; Sangkham, S.; Jirapornkul, C.; Limmongkon, Y.; Daduang, S.; Tessiri, T.; Rayubkul, J.; Thongtip, S.; Maneenin, N.; et al. Human health risk assessment of $PM_{2.5}$-bound heavy metal of anthropogenic sources in the Khon Kaen Province of Northeast Thailand. *Heliyon* **2022**, *8*, e09572. [CrossRef]
30. Kanchanasuta, S.; Sooktawee, S.; Patpai, A.; Vatanasomboon, P. Temporal variations and potential source areas of fine particulate matter in Bangkok, Thailand. *Air Soil Water Res.* **2020**, *13*, 1178622120978203. [CrossRef]
31. Bhuyan, P.; Barman, N.; Begum, S.; Gogoi, D.; Borah, S.; Kumar, M.; Sarma, K.P.; Hoque, R.R. Spatial and seasonal variations of Water-soluble ions in PM_{10} of Mid-Brahmaputra plain of Assam valley. *Asian J. Water Environ. Pollut.* **2016**, *13*, 69–81. [CrossRef]
32. Thammasaroj, P.; Jinsart, W. Effects of overcrowded traffic and road construction activities in Bangkok on $PM_{2.5}$, PM_{10}, and heavy metals composition. *Environ. Asia* **2019**, *12*, 28–35.
33. Han, Y.M.; Cao, J.J.; Lee, S.C.; Ho, K.F.; An, Z.S. Different characteristics of char and soot in the atmosphere and their ratio as an indicator for source identification in Xi'an, China. *Atmos. Chem. Phys.* **2010**, *10*, 595–607. [CrossRef]
34. Shen, Z.; Han, Y.; Cao, J.; Tian, J.; Zhu, C.; Liu, S.; Liu, P.; Wang, Y. Characteristics of traffic-related emissions: A case study in roadside ambient air over Xi'an, China. *Aerosol Air Qual. Res.* **2010**, *10*, 292–300. [CrossRef]
35. Begum, B.A.; Biswas, S.K.; Markwitz, A.; Hopke, P.K. Identification of sources of fine and coarse particulate matter in Dhaka, Bangladesh. *Aerosol Air Qual. Res.* **2010**, *10*, 345–353. [CrossRef]
36. Kumar, P.; Yadav, S. Seasonal variations in water-soluble inorganic ions, OC and EC in PM_{10} and $PM_{>10}$ aerosols over Delhi: Influence of sources and meteorological factors. *Aerosol Air Qual. Res.* **2016**, *16*, 1165–1178. [CrossRef]
37. Liu, W.; Xu, Y.; Liu, W.; Liu, Q.; Yu, S.; Liu, Y.; Wang, X.; Tao, T. Oxidative potential of ambient $PM_{2.5}$ in the coastal cities of the Bohai sea, northern China: Seasonal variation and source apportionment. *Environ. Pollut.* **2018**, *236*, 514–528. [CrossRef] [PubMed]
38. Lv, B.; Zhang, B.; Bai, Y. A systematic analysis of $PM_{2.5}$ in Beijing and its sources from 2000 to 2012. *Atmos. Environ.* **2016**, *124 Pt B*, 98–108. [CrossRef]
39. Liang, Z.; Zhao, X.; Chen, J.; Gao, L.; Zhu, A.; Wang, Z.; Li, S.; Shan, J.; Long, Y.; Yan, C.; et al. Seasonal characteristics of chemical compositions and sources identification of $PM_{2.5}$ in Zhuhai, China. *Environ. Geochem. Health* **2018**, *41*, 715–728. [CrossRef]

40. Tsai, J.H.; Lin, J.H.; Yao, Y.C.; Chiang, H.L. Size distribution and water-soluble ions of ambient particulate matter on the episode and non-episode days in Southern Taiwan. *Aerosol Air Qual. Res.* **2012**, *12*, 263–274. [CrossRef]
41. Zhang, L.; Vet, R.; Wiebe, A.; Mihele, C.; Sukloff, B.; Chan, E.; Moran, M.D.; Iqbal, S. Characterization of the size-segregated water-soluble inorganic ions at eight Canadian rural sites. *Atmos. Chem. Phys.* **2008**, *8*, 7133–7151. [CrossRef]
42. Kim, I.G.; Jo, B.H.; Kang, D.G.; Kim, C.S.; Choi, Y.S.; Cha, H.J. Biomineralization-based conversion of carbon dioxide to calcium carbonate using recombinant carbonic anhydrase. *Chemosphere* **2012**, *87*, 1091–1096. [CrossRef]
43. Rastogi, N.; Singh, A.; Sarin, M.M.; Singh, D. Temporal variability of primary and secondary aerosols over northern India: Impact of biomass burning emissions. *Atmos. Environ.* **2016**, *125*, 396–403. [CrossRef]
44. Yadav, S.; Rajamani, V. Geochemistry of aerosols of the north-western part of India adjoining the Thar Desert. *Geochim. Cosmochim. Acta* **2004**, *68*, 1975–1988. [CrossRef]
45. Kumar, S.; Aggarwal, S.G.; Gupta, P.K.; Kawamura, K. Investigation of the tracers for plastic-enriched waste burning aerosols. *Atmos. Environ.* **2015**, *108*, 49–58. [CrossRef]
46. Li, L.; Li, M.; Huang, Z.; Gao, W.; Nian, H.; Fu, Z.; Gao, J.; Chai, F.; Zhou, Z. Ambient particle characterization by single particle aerosol mass spectrometry in an urban area of Beijing. *Atmos. Environ.* **2014**, *94*, 323–331. [CrossRef]
47. Pant, P.; Harrison, R.M. Critical review of receptor modeling for particulate matter: A case study of India. *Atmos. Environ.* **2012**, *49*, 1–12. [CrossRef]
48. Mansha, M.; Ghauri, B.; Rahman, S.; Amman, A. Characterization and source apportionment of ambient air particulate matter ($PM_{2.5}$) in Karachi. *Sci. Total Environ.* **2012**, *425*, 176–183. [CrossRef]
49. Klimaszewska, K.; Polkowska, Ż.; Namieśnik, J. Influence of mobile sources on pollution of runoff waters from roads with high traffic intensity. *Pol. J. Environ. Stud.* **2007**, *16*, 889–897.
50. Hu, X.; Zhang, Y.; Ding, Z.H.; Wang, T.J.; Lian, H.Z.; Sun, Y.Y.; Wu, J. Bio-accessibility and health risk of arsenic and heavy metals (Cd Co, Cr, Cu, Ni, Pb, Zn and Mn) in TSP and $PM_{2.5}$ in Nanjing, China. *Atmos. Environ.* **2012**, *57*, 146–152. [CrossRef]
51. Diaz, R.V.; Dominguez, E.R. Health risk by inhalation of $PM_{2.5}$ in the metropolitan zone of the city of Mexico. *Ecotoxicol. Environ. Saf.* **2009**, *72*, 866–871. [CrossRef]
52. Yadav, S.; Satsangi, P.G. Characterization of particulate matter and its related metal toxicity in an urban location in South West India. *Environ. Monit. Assess.* **2013**, *185*, 7365–7379. [CrossRef]
53. Zhang, N.; Han, B.; He, F.; Xu, J.; Niu, C.; Zhou, J.; Kong, S.; Bai, Z.; Xu, H. Characterization, health risk of heavy metals, and source apportionment of atmospheric $PM_{2.5}$ to children in summer and winter: An exposure panel study in Tianjin, China. *Air Qual. Atmos. Health* **2015**, *8*, 347–357. [CrossRef]
54. Srimuruganandam, B.; Nagendra, S.S. Source characterization of PM_{10} and $PM_{2.5}$ mass using a chemical mass balance model at the urban roadside. *Sci. Total Environ.* **2012**, *433*, 8–19. [CrossRef] [PubMed]
55. Srimuruganandam, B.; Nagendra, S.S. Application of positive matrix factorization in the characterization of PM_{10} and $PM_{2.5}$ emission sources at the urban roadside. *Chemosphere* **2012**, *88*, 120–130. [CrossRef] [PubMed]
56. Kothai, P.; Saradhi, I.V.; Prathibha, P.; Hopke, P.K.; Pandit, G.G.; Puranik, V.D. Source apportionment of coarse and fine particulate matter at Navi Mumbai, India. *Aerosol Air Qual. Res.* **2008**, *8*, 423–436.
57. Sharma, S.K.; Mandal, T.K.; Srivastava, M.K.; Chatterjee, A.; Jain, S.; Saxena, M.; Singh, B.P.; Sharma, A.; Adak, A.; Ghosh, S.K. Spatio-temporal variation in chemical characteristics of PM_{10} over Indo Gangetic plain of India. *Environ. Sci. Pollut. Res.* **2016**, *23*, 18809–18822. [CrossRef]
58. Marmur, A.; Unal, A.; Mulholland, J.A.; Russell, A.G. Optimization-based source apportionment of $PM_{2.5}$ incorporating gas-to-particle ratios. *Environ. Sci. Technol.* **2005**, *39*, 3245–3254. [CrossRef]
59. Andersen, Z.J.; Wahlin, P.; Raaschou-Nielsen, O.; Scheike, T.; Loft, S. Ambient particle source apportionment and daily hospital admissions among children and elderly in Copenhagen. *J. Expo. Sci. Environ. Epidemiol.* **2007**, *17*, 625–636. [CrossRef]
60. Khare, P.; Baruah, B.P. Elemental characterization and source identification of $PM_{2.5}$ using multivariate analysis at the suburban site of northeast India. *Atmos. Res.* **2010**, *98*, 148–162. [CrossRef]